Climate Dynamics (2004) 22: 327–341
DOI 10.1007/s00382-003-0375-8

A. C. Clement · A. Hall · A. J. Broccoli

The importance of precessional signals in the tropical climate

Received: 26 March 2003 / Accepted: 6 October 2003 / Published online: 27 February 2004

Abstract Past research on the climate response to orbital forcing has emphasized the glacial-interglacial variations in global ice volume, global-mean temperature, and the global hydrologic cycle. This emphasis may be inappropriate in the tropics, where the response to precessional forcing is likely to be somewhat independent of the glacial-interglacial variations, particularly in variables relating to the hydrologic cycle. To illustrate this point, we use an atmospheric general circulation model coupled to a slab ocean model, performing experiments that quantify the tropical climate's response to (1) opposite phases of precessional forcing, and (2) Last Glacial Maximum boundary conditions. While the glacially-forced tropical temperature changes are typically more than an order of magnitude larger than those arising from precessional forcing, the hydrologic signals stemming from the two forcings are comparable in magnitude. The mechanisms behind these signals are investigated and shown to be quite distinct for the precessional and glacial forcing. Because of strong dynamical linkages in the tropics, the model results illustrate the impossibility of predicting the local hydrologic response to external forcing without understanding the response at much larger spatial scales. Examples from the paleoclimate record are presented as additional evidence for the importance of precessional signals in past variations of the tropical climate.

A. C. Clement (✉)
Rosenstiel School of Marine and Atmospheric Science,
University of Miami, 4600 Rickenbacker Causeway, Miami,
FL 33149, USA
E-mail: aclement@rsmas.miami.edu

A. Hall
UCLA, 7955 Math Sciences Building, 405 Hilgard Ave.,
Box 951565, Los Angeles, CA 90095, USA

A. J. Broccoli
Rutgers University, 14 College Farm Road, New Brunswick,
NJ 08901-8551, USA

1 Introduction

A major question in paleoclimate research is why the glaciations and the associated changes in global mean temperature of the late Pleistocene recur approximately every 100-kyears (kys). Milankovitch (1920) proposed that ice ages occur when the Earth's orbit is configured so that the Northern Hemisphere receives less solar insolation in summer, leading to growth of the northern ice sheets. It is now clear that global ice volume variations are indeed somehow paced by changes in the Earth's orbital parameters (Hays et al. 1976; Imbrie et al. 1992). However, basic questions remain about the orbital-climate connection. The changes in orbital parameters redistribute solar insolation seasonally and latitudinally without changing the global mean insolation signifcantly, making the large excursions of global mean temperature difficult to explain. It is also difficult to account for the large amplitude of the ice volume and global mean temperature variations on the 100 kyr time scale, since the orbital forcing is dominated by the 20 and 40 kyr time scales (Imbrie et al. 1993).

Numerous global-scale feedbacks in the climate system have been hypothesized to explain changes in the global mean temperature between glacials and interglacials. These include ice albedo feedbacks, changes in the ocean circulation, atmospheric greenhouse gas and dust concentrations (see e.g., Broecker 1995). Unfortunately, little concrete evidence to support these hypotheses is available. Consequently, much effort has gone into examining the linkages between regional climates worldwide and the glacial-interglacial cycle in the hope that some undiscovered teleconnection could be the reason for it. Perhaps the most influential effort to support this view has been the SPECMAP project (Imbrie et al. 1984). Those authors compiled marine records from around the globe to establish a common chronology of glacial-interglacial change, using the fact that as ice accumulates on land, the proportion of

heavier oxygen isotopes increases throughout the global ocean. It is now standard practice to compare new records with that chronology, placing emphasis on the globally correlated part of climate records. This view does not require everything to be synchronized throughout the globe. Rather, discrepancies in the timing of local or regional changes relative to the ice volume are often interpreted as leading or lagging the glacial-interglacial cycle, and not as distinct climate signals.

In this study, we highlight a potential difficulty with this approach to the orbital-climate problem namely: though the glacial-interglacial cycle may have a prominent signal worldwide, the regional response to the direct solar forcing may also be large and have a significantly different character. A test of this idea is critical for the interpretation of paleoclimate records. For example, if a regional record differs from the global ice volume record (e.g., SPECMAP), the difference may not represent a lead or lag, but instead a regional climate signal resulting from direct local orbital forcing that is quite independent of glacial-interglacial cycle. In the extreme, the regionally based orbital signal could overwhelm the remotely forced glacial-interglacial signal leading to a gross misinterpretation of the record.

The goal of this study is to unravel this ambiguity by quantifying the orbitally driven local climate variations and the local signatures of the global scale glacial-interglacial cycle in a numerical model of the climate system. By exploring the mechanisms that are responsible for these two sources of climate variations, we also aim to provide a physical basis for interpretation of tropical paleoclimate records. To do this, we make a somewhat artificial distinction between 'glacial' and 'precessional' forcing, and take the former to represent the fluctuations in ice volume, CO_2, and sea level that recur mainly every 100-kyr, while the latter is strictly the change in insolation arising from the precession of the equinoxes. (We focus on the precessional forcing here because of its large magnitude in the tropics; obliquity is discussed in the final section.) There is no doubt some interaction between the mechanisms that operate in response to the glacial and precessional forcings, since ultimately the orbital forcing is believed to cause glacial-interglacial fluctuations. However, the climate responses must be somewhat distinct. For example, Shackleton (2000) showed that atmospheric CO_2 and deep ocean temperature are strongly linked only on the 100-kyr time scale. He argued that this implies a feedback between climate and the global carbon cycle that operates on the 100-kyr time scale, but does not appear to control ice volume on shorter orbital time scales.

In Sect. 2, we describe our modeling approach in more detail. In Sect. 3, we advance a picture of the large-scale patterns in temperature and precipitation associated with the glacial and precessional forcings. Section 4 delves into mechanisms that give rise to the large-scale seasonal patterns of the climate's response to these forcings. Section 5 discusses the limitations of the present model arrangement. In Sect. 6, we use the modeling results and paleoclimate examples to illustrate the implications of our results for the interpretation of the paleoclimate record.

2 Methodology

Numerous modeling studies of the climate response to the late Quaternary external forcings have been performed using general circulation models (GCMs) of a range of complexity. This range encompasses atmospheric GCMs forced by specified sea surface temperatures as the lower boundary condition, atmospheric GCMs coupled to mixed-layer ocean models, and coupled ocean–atmosphere GCMs. To test the Milankovitch hypothesis much previous effort has been into understanding the orbital controls on the conditions for Northern Hemisphere glaciation (Rind et al. 1989; Phillips and Held 1994; Harrison et al. 1995; Khodri et al. 2001). Another issue that has received attention from the climate modeling community is the climatic response to glacial boundary conditions (Hewitt and Mitchell 1997; Broccoli and Manabe 1987; Broccoli 2000; Pinot et al. 1999; Hewitt et al. 2001). The results are often compared with the available climate proxies from the Last Glacial Maximum (LGM) to evaluate the feedback mechanisms and climate sensitivity. A third focus has been the response of Northern Hemisphere monsoons to orbital forcing and glacial conditions (Kutzbach et al. 1977; Prell and Kutzbach 1987; Kutzbach and Liu 1997; Joussaume et al. 1999). Such studies investigate regional circulations during a particular season and how these compare with available monsoon paleoclimate proxies. As stated in the Introduction, the focus of our study is on the global tropics.

The climate model we use for our investigation consists of three components: (1) an atmospheric general circulation model (GCM), (2) a heat and water balance model over the continents and (3) a simple mixed layer ocean model. The atmosphere is run at R30 resolution, which corresponds to a grid spacing of approximately 2.25° latitude × 3.75° longitude, with 20 vertical levels. The ocean mixed-layer is treated as a static layer 50 m deep whose temperature is uniform with depth. To represent the horizontal heat transport by ocean currents an additional heat flux term is applied in the ocean that varies geographically and seasonally, but not from year to year. See Broccoli (2000) for additional model details. We note that this model arrangement does not account for the effect of interactive ocean dynamics on the heat budget of the mixed layer, a limitation we discuss in Sect. 5.

Experiments are performed to test the tropical climate response to glacial and precessional forcing. For the glacial response, we analyze an experiment designed to simulate the LGM climate, as described in detail in Broccoli (2000). The forcing is specified by Paleoclimate Modelling Intercomparison Project (PMIP) as: Peltier (1993) paleotopography (ICE-4G) with the implied sea level reduction of 105 m; 21 K orbital parameters (Berger (1978); CO_2 reduced to 200 ppmv; no change in surface albedo of snow-free and ice-free land. This run is referred to as LGM. The LGM represents one extreme phase of the glacial-interglacial cycle, and is compared with the other extreme, the modern interglacial. For the precessional response, a model run is performed in which the longitude of perihelion is shifted 180 degrees out of phase with the modern, with eccentricity and other boundary conditions set to modern values (P + 180). While this is only one phase of the precessional forcing, it represents the largest difference in phasing from the modern configuration and corresponds approximately to the precessional forcing at 11 ka. The climatic precession is the product of both the eccentricity and the actual precession of the equinoxes. The modern eccentricity is relatively low. Jackson and Broccoli (2003) found that the response of many climate variables is nearly linear with respect to eccentricity, and one would thus expect that at times of higher eccentricity (e.g., during the early glacial), the precessional signal would have been considerably larger.

The results from these experiments are compared with a control run in which CO_2 is set at its pre-industrial level of 280 ppmv (CTRL). Thus, here the term 'modern' refers to the pre-industrial

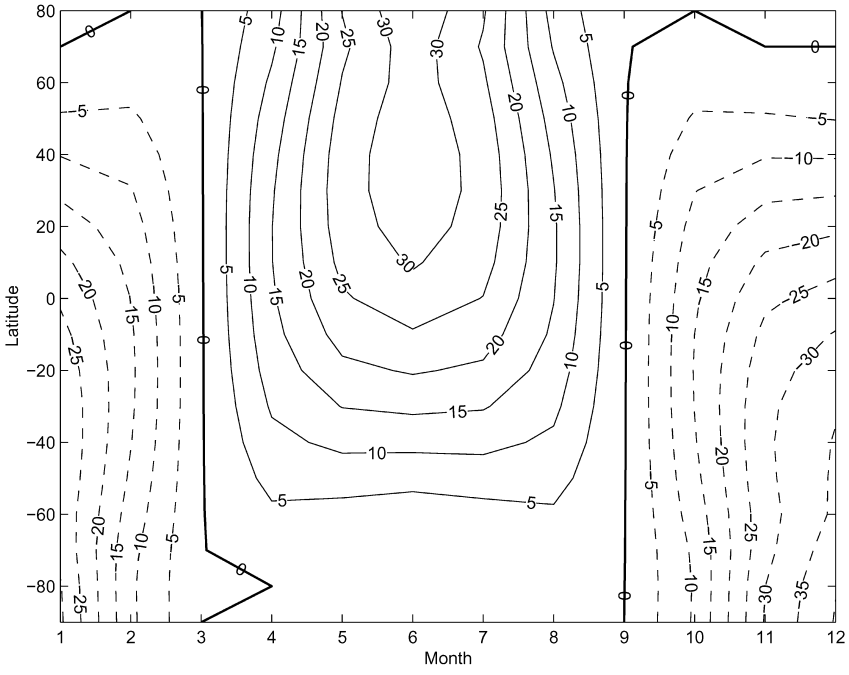

Fig. 1 Latitude, month plot of the change in top-of-atmosphere insolation due to a 180-degree shift in the longitude of perihelion relative to the modern in Wm^{-2} used for the P + 180 run. The contour interval is 5 Wm^{-2}

climate. All runs are 30 years long, resulting in stable climatologies. Each year of the model is defined to have 365 days with a fixed vernal equinox on March 21st in accordance with PMIP (Joussaume and Taylor 1995). Because the rate of change of the seasons depends on the longitude of the perihelion, seasonal information may be distorted slightly by a "calendar effect" (Joussaume and Braconnot 1997). For reference, Fig. 1 shows the seasonal and latitudinal structure of the precessional forcing, expressed as changes in the incident top-of-atmosphere solar radiation.

3 Annual mean overview

To provide an overview of the model's response to glacial and orbital forcings, we first present the simulated responses in annual mean zonal mean temperature (Fig. 2) and precipitation (Fig. 3). We focus on the zonal mean to produce the first order picture of temperature and hydrological cycle changes. The glacial signal in temperature is an order of magnitude larger than the precessional signal. There also is a significant change in the meridional gradient in the glacial case. This is due to a combination of two factors: (1) the presence of highly reflective Northern Hemisphere ice sheets which reduce the net incoming shortwave radiation at high northern latitudes, and (2) the reduction in CO_2 which leads to a cooling that is amplified at high latitudes in both hemispheres. Most of the temperature change in the tropics is related to the reduction in CO_2 with a small additional contribution from the ice sheet in the Northern Hemisphere tropics (A.J. Broccoli personal communication). Greater sensitivity in high latitudes to a globally distributed uniform forcing has been noted in many climate change simulations, and results from positive feedbacks involving snow and sea ice, and the greater static stability in polar regions which confines the effects of perturbations in the surface energy balance to a relatively shallow layer (e.g., Manabe and Stouffer 1980; Hall 2003). In the precessional case, the forcing itself has little meridional gradient in the annual mean (Fig. 1), and the small meridional gradient in the response is due mainly to the positive sea ice and snow feedbacks noted.

Viewed on its own, the temperature response shown in Fig. 2 would suggest that the glacial signal should dominate paleoclimate proxies. Also, it would suggest that the tropical climate exhibits very little sensitivity to precessional forcing. However, an examination of the response of the tropical hydrology reveals that this is not the case (Fig. 3). The most striking feature here is that, while the magnitude of the glacial temperature signal is more than an order of magnitude larger than the precessional signal, the glacial and precessional precipitation signals are comparable in magnitude. In the early glacial when eccentricity is larger than that used in the P + 180 experiment (not shown), the magnitude of the precessional precipitation signal would likely even exceed that of the glacial.

The hemispheric asymmetry of the precipitation response is striking in both the glacial and precessional cases. In the glacial case, the response is more zonally symmetric in the sense that precipitation changes over land are the same sign as changes over the ocean. In the global mean, precipitation decreases in response to the glacial forcing. This occurs because atmospheric temperatures are reduced throughout the globe (Fig. 2a). In global warming scenarios, the hydrological cycle speeds up (Manabe and Wetherald 1975; Mitchell et al. 1995; Hall and Manabe 2000), which is the reverse of what is shown here in association with the global cooling in the glacial. An exception to this global pattern is the precipitation increase to the south of the equator. A similar

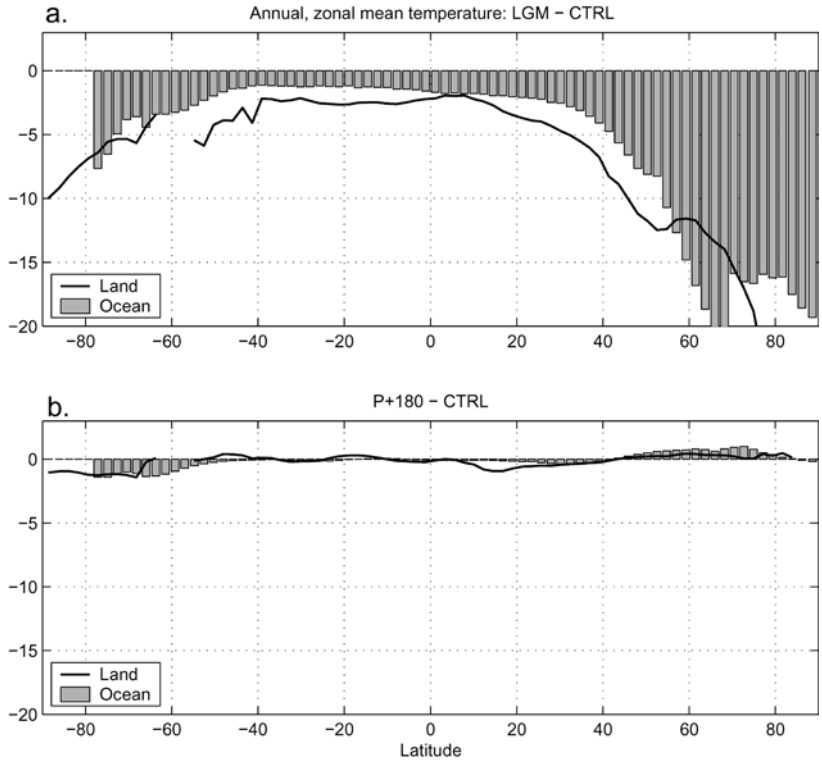

Fig. 2 **a** Zonal mean, annual mean surface temperature change over land (*solid line*) and ocean (*gray bars*) as a function of latitude due to glacial forcing (LGM–CTRL) **b** Same as **a** but for P + 180–CTRL

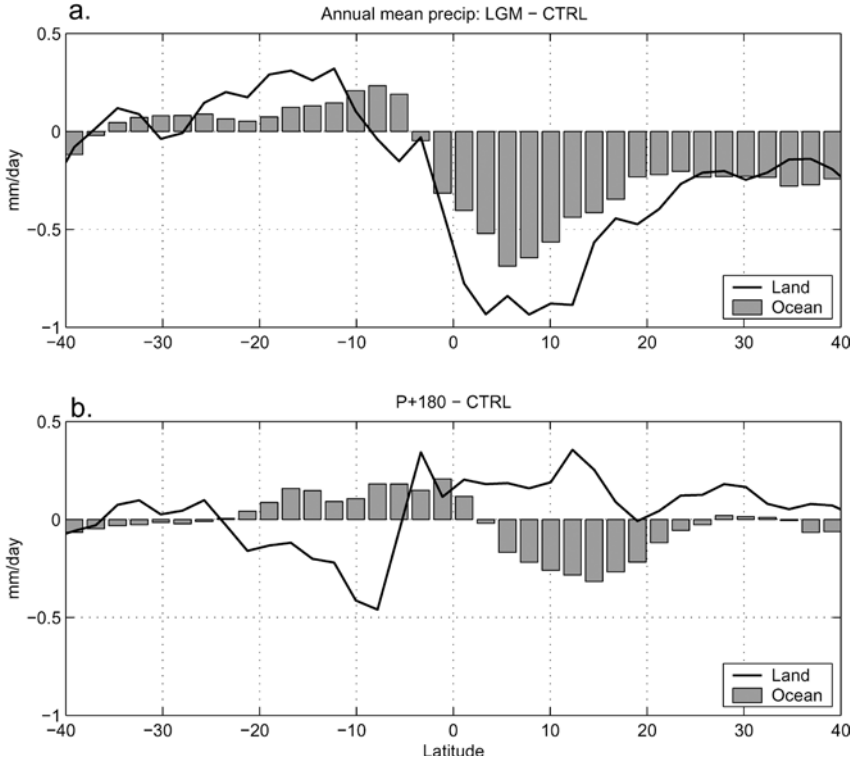

Fig. 3 **a** Zonal mean, annual mean precipitation change over land (*solid line*) and ocean (*gray bars*) as a function latitude in mm/day due to glacial forcing (LGM–CTRL) in the tropics only. **b** Same as **a** but for P + 180–CTRL

meridional structure in the glacial precipitation response can be seen in models of varying complexity (Pinot et al. 1999; Ganopolski et al. 1998). This is an important dynamical signature that will be discussed in the next section. In clear contrast to the glacial case, for the precessional forcing there are significant zonal asymmetries

in the precipitation response with out-of-phase changes over land and ocean (Fig. 3b). We shall see that this is a characteristic of the dynamical response of the tropical atmosphere to precessional forcing. In addition to being clues to the dynamical mechanisms underlying the hydrologic response to external forcing, these large-scale patterns in precipitation are important in understanding linkages between paleoclimate observations in different regions of the tropics. This will be discussed in Sect. 5.

4 Seasonal forcing and response

4.1 Climatology of the simulated tropical circulation

In the tropics, the large-scale circulation can be described in large part as made up of the Hadley and Walker cells and regional monsoons (Trenberth et al. 2000). These circulations have the important effect of linking together large regions of the tropics through well-studied physical mechanisms in both the zonal and meridional directions. In this section, we show that the tropical circulations are reasonably well simulated in the CTRL run, and describe the mechanisms that play an important role in maintaining the present-day tropical circulation, and also in the tropical response to glacial and precessional forcing.

To visualize the simulated large-scale tropical circulation it is useful to divide the velocity field into a non-divergent (rotational or quasi-geostrophic) part and a divergent part: $\boldsymbol{v} = \boldsymbol{v}_\psi + \boldsymbol{v}_\varphi = \boldsymbol{k} \times \nabla\psi + \nabla\varphi$ where φ is the velocity potential and ψ is the stream function. The divergent part of the circulation reflects the flow into and out of heat sources and sinks. In the lower troposphere, flow converges into a region of heating, while in the upper troposphere, the flow diverges from the region. The Hadley, Walker and monsoon circulations are thermally driven so that their signatures appear most clearly in the divergent part of the circulation.

Figures 4a and 9a show the boreal winter and summer precipitation and divergent wind for the control run averaged over three sigma levels corresponding to approximately the 200 to 330 hPa range. These are the levels where the mean upper tropospheric wind reaches its maximum. (The glacial and precessionally forced anomalies also reach their maxima at these levels). In DJF (Fig. 4a) the main areas of upper tropospheric wind divergence (heating and precipitation) are south of the equator, and convergence generally occurs to the north of the equator. In the zonal mean, this is the Hadley circulation with ascent in the southern tropics, southerly cross-equatorial flow aloft and sinking in the north (Fig. 5a). This circulation arises from the meridional gradient in solar forcing which causes lower tropospheric temperature to be maximum in the southern hemisphere (Fig. 6a). (The spatial pattern of surface temperature looks very similar to that of lower tropospheric temperature, but with some additional smaller scale features that we are not interested in here.) It is clear from Fig. 4a, however, that the circulation does not look Hadley-like at all longitudes, and that the strongest cross-equatorial flow occurs in the sectors where precipitation is strongest in the southern hemisphere.

These longitudinal differences arise from the zonal structure in SST, the land-sea contrast in surface temperature and topography. Rodwell and Hoskins (2001) have suggested this longitudinal structure results from off-equatorial heating over land which has a remote response via linear waves both to the east and west of the continents. To the west of the heating region, a Rossby wave response produces adiabatic descent, which contributes to the strength of the subsidence over the eastern ocean basins. To the east, there is a Kelvin wave response. This strengthens the tropical easterlies in that ocean basin on the equatorward flank of the subtropical anticyclone and strengthens the high pressure system. Thus, during the austral summer, high topography over the Andes and high temperatures over the S. American continent (Fig. 6a) produce convection in the regions, which by the arguments of Rodwell and Hoskins (2001), leads to subsidence over both the subtropical South Atlantic and eastern South Pacific.

In JJA, the Hadley circulation is reversed and the main areas of convection and upper tropospheric divergence shift to the Northern Hemisphere, while the subsidence shifts to the southern subtropics (Figs. 9a, 10a). Here the zonal asymmetries are also quite pronounced with the main heat source occurring in the Asian-Pacific region. Several authors have now argued that this heat source alone can explain the main features of the Northern Hemisphere summer subtropical climate. The work of Rodwell and Hoskins (1996, 2001) demonstrated that the dryness of Mediterranean climate, and the strength of the north Pacific subtropical high could be related to the Asian monsoon heating. Chen et al. (2001) went further to suggest on the basis of model results that the subtropical highs of both the Pacific and Atlantic owe their existence to propagation of Rossby waves from the heat sources over Asia.

4.2 Response to glacial and precessional forcing in austral summer

With this view of the seasonal climatology and some of the mechanisms that generate it, we now diagnose how the atmospheric circulation is altered by the glacial and precessional forcings, considering first the austral summer (DJF) responses. Figure 4b shows the change in the divergent wind and precipitation between the glacial run and the control. This is an intensification of the main centers of convection in the modern climate (Fig. 4a), which are the regional contributions to the rising branch of the Hadley circulation. In the western Pacific, there is also a shift to the south of the maximum precipitation which is evidenced by the increase in

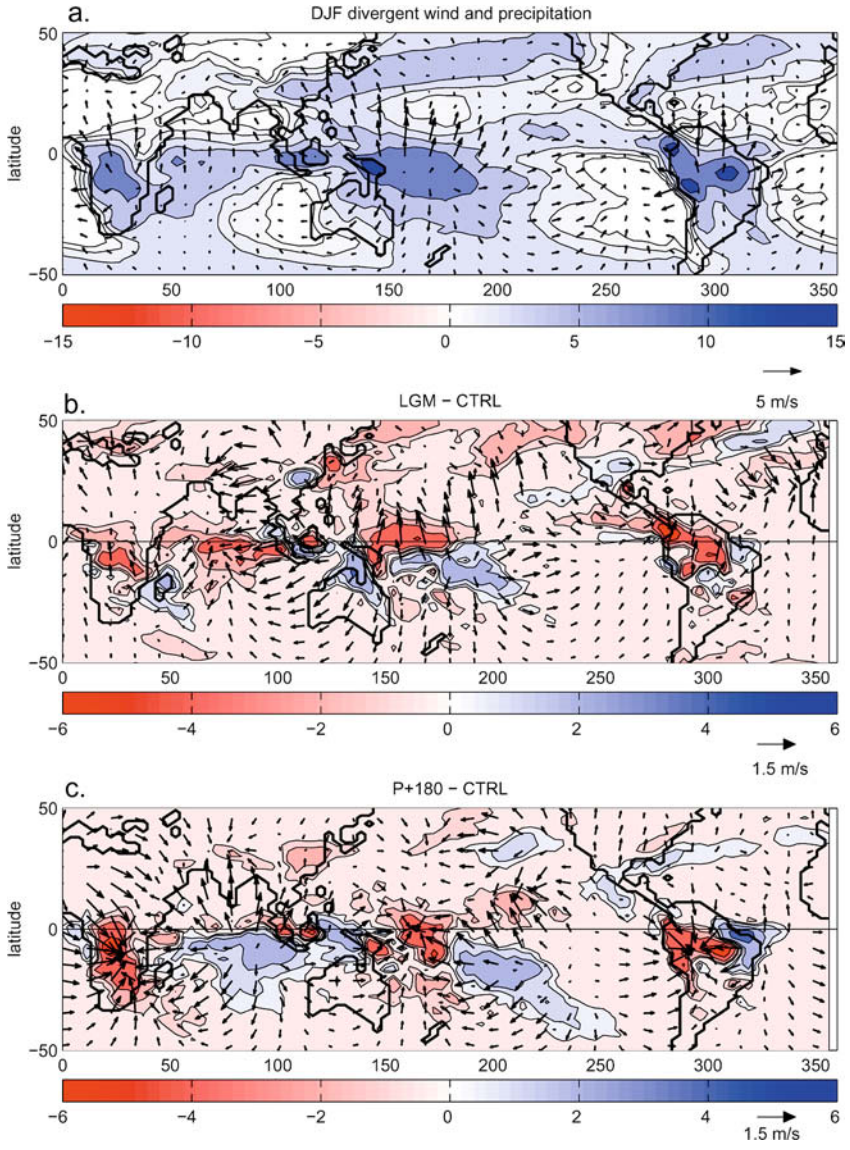

Fig. 4 DJF precipitation (*colors* and *contours*, mm/day) and upper tropospheric divergent winds (*vectors*, m/s) for **a** CTRL, **b**LGM–CTRL, **c** P + 180–CTRL. The contour interval for precipitation is logarithmic with values. The zero contour is not drawn in all panels to improve clarity

precipitation south of the equator and the decrease on the equator. In the zonal mean, this anomalous circulation is an intensification and a southward shift of the boreal winter Hadley cell (Fig. 5b). Broccoli (manuscript in preperation) has shown that this response is related to the change in meridional gradients associated with the glacial forcing, since the first order change in the lower tropospheric temperature is the larger cooling of the Northern Hemisphere relative to the south (Fig. 6b). This is also consistent with the mechanism proposed by Lindzen and Hou (1988) and Lindzen and Pan (1994) whereby a shift off the equator of the latitude of maximum heating results in a stronger Hadley circulation. In the glacial, because of the warmth of the Southern Hemisphere relative to the north, the maximum SSTs are shifted further to the south of the equator and the DJF Hadley cell increases in strength.

Although there is a rough correspondence between the glacially forced anomalies in the divergent circulation and precipitation, it is the convergence of water vapor, not mass, that precisely balances evaporation and precipitation. By analyzing the balance equation for water vapor, we can evaluate the relationship between circulation and precipitation changes more rigorously. The vertical integral of the water vapor budget averaged over a season (so that the storage term is negligible) can be written as:

$$\frac{1}{g}\int \nabla \cdot (q2v)\mathrm{d}p = E - P \qquad (1)$$

where q is the specific humidity, $\boldsymbol{v}$ is the vector horizontal wind, E is the evaporation and P is the precipitation. Since we are interested in changes relative to the modern state, we can linearize the humidity and wind changes as: $q = \bar{q} + q'$and $v = 2\bar{v} + 2v'$ (and similarly for evaporation and precipitation). Then we can rewrite Eq. (1), removing the mean (modern) field as:

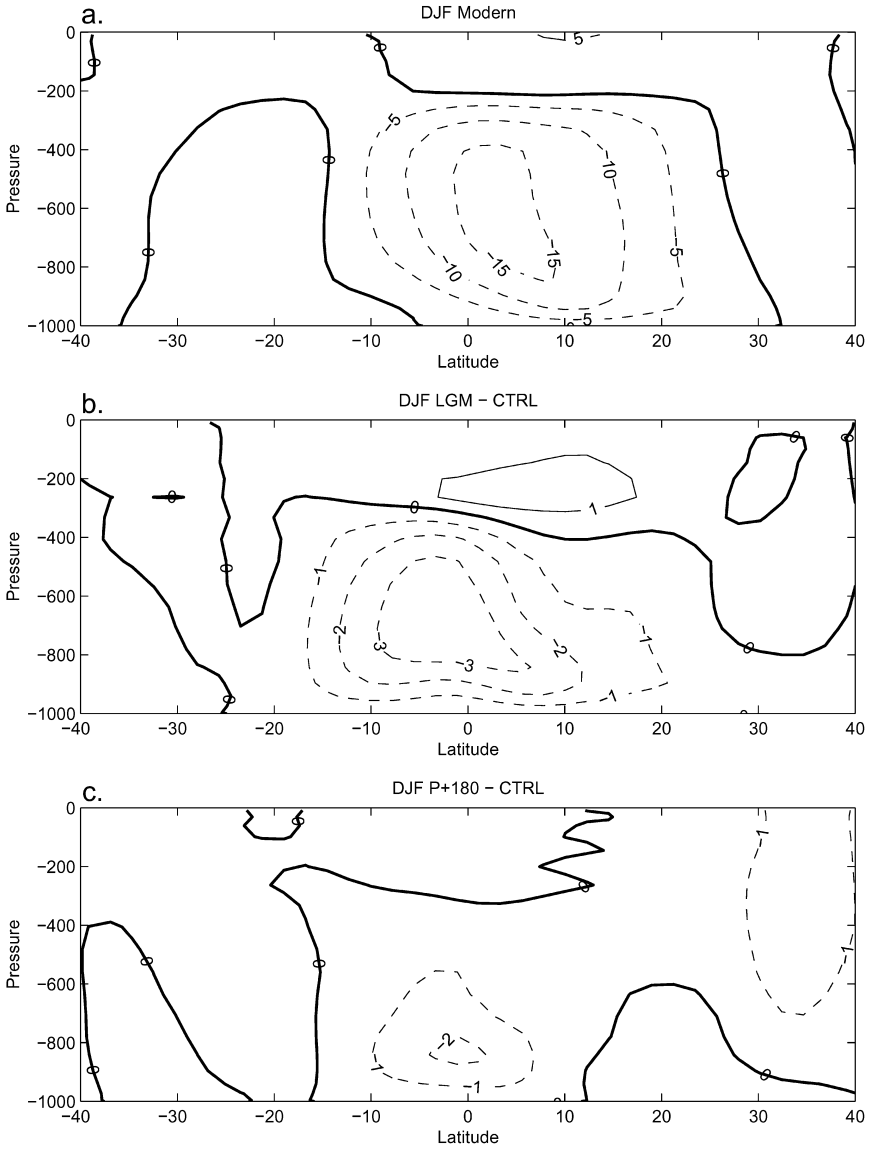

Fig. 5 DJF zonal mean meridional stream function (10^{10} kg/s) for **a**CTRL, **b** LGM–CTRL, **c** P + 180–CTRL

$$P' = \underbrace{E'}_{\text{I}} - \frac{1}{g}\int [\underbrace{\nabla \cdot (\bar{q}\ 2v')}_{\text{II}} + \underbrace{\nabla \cdot (q'\ 2\bar{v})}_{\text{III}} + \underbrace{\nabla \cdot (q'\ 2v')}_{\text{IV}}]\mathrm{d}p \tag{2}$$

This linearization allows us to separate the effects on the precipitation field of the circulation changes (term II) and changes in the mean humidity field (term III), and the cross term (term IV) which is small. We note that by using seasonal mean quantities, we are neglecting the contribution of transient eddies to the moisture balance. By comparing the left and right-hand sides of Eq. (2), we find that this contribution is negligible in the perturbed climates (not shown). Figure 7 shows terms II and III for the glacial DJF case. The pattern of term II compares quite well with the precipitation changes shown in Fig. 4b, which suggests that circulation changes largely explain the precipitation response to glacial forcing. However, there is a significant contribution to the water vapor balance by the mean divergence of the anomalous humidity field (term III, Fig. 7b). The large cooling throughout the tropics leads to a widespread reduction in humidity. Consequently, the reduction in water vapor convergence is largest in regions where the water vapor convergence, and therefore precipitation, is largest in the unperturbed climate (Fig. 4a). Thus, the glacial signal consists of both a dynamical signal that shifts precipitation to the south, and a mean reduction of precipitation with a spatial pattern that is similar to the unperturbed field.

The precessional response is shown in Fig. 4c. The zonal structure of the divergent circulation response is striking. In the P + 180 experiment, the Earth is further from the Sun in DJF than it is in CTRL. (In the modern climate perihelion occurs at the beginning of January, while a shift in perihelion by 180 degrees means that

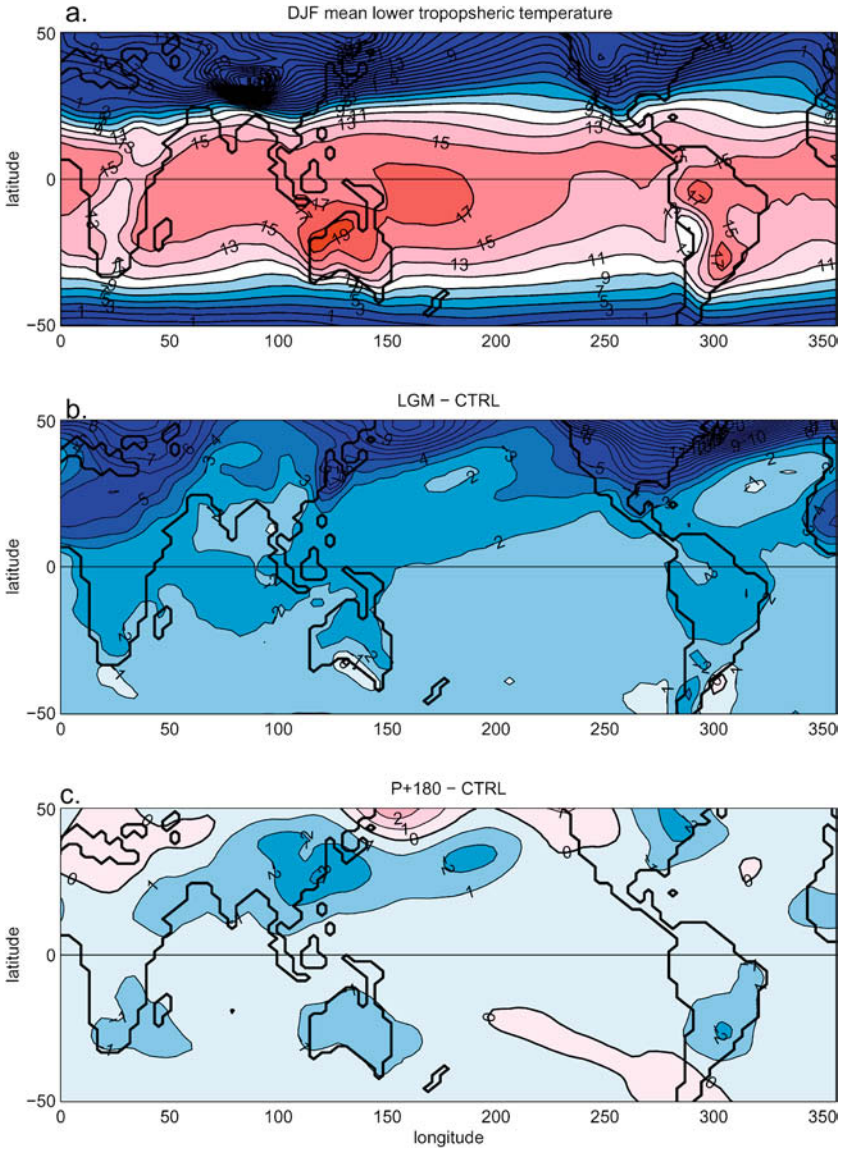

Fig. 6 DJF lower tropopsheric temperature (averaged over 1000–500 hPa) for **a** CTRL. *Contour interval* is 2 K. **b** LGM–CTRL. **c** P + 180–CTRL. The *contour interval* is 1 K in **b** and **c**

aphelion occurs at that time.) The larger Earth–Sun distance reduces the insolation (see Fig. 1), resulting in a small cooling throughout most of the tropics (Fig. 6c). However, because of the lower heat capacity of land relative to ocean, the cooling is not uniform. The land cools by more, reducing the land-sea temperature contrast in the Southern Hemisphere. As a result, the main centers of convection over land in southern Africa and S. America are weakened (Fig. 4c). Regions of increased upper tropospheric divergence are also evident from Fig. 4c over the eastern tropical Pacific, the central Indian Ocean and the South Atlantic. This is consistent with the work of Rodwell and Hoskins (2001), from which it follows that a weaker heat source over land, as is the case here, would have weaker subsidence over the oceans both to the east and the west of the continents. Though Rodwell and Hoskins (2001) studied the response to a single heat source in a purely dynamical model, it is clear that mechanisms in our model are roughly analogous. The result of this change in circulation is in a general shift of precipitation from the land to the ocean in the Southern Hemisphere, which explains the zonal mean patterns of Fig. 3b. Though relevant for the glacial case, the mechanism proposed by Lindzen and Pan (1994) for modulation of the Hadley cell by precessional forcing is unlikely to be important in this season, since the change in the zonal mean circulation (Fig. 5c) does not extend through much of the troposphere, and is small compared to the zonally asymmetric circulation changes.

Figure 8 shows that the precessional precipitation changes, unlike their glacial counterparts, are almost entirely driven by circulation changes. Both the pattern and amplitude of term II correspond very well to the precipitation changes shown in Fig. 4c, while term III is very small and bears little relationship to those precipitation changes. Term III is so small because of the relatively small changes in temperature forced by

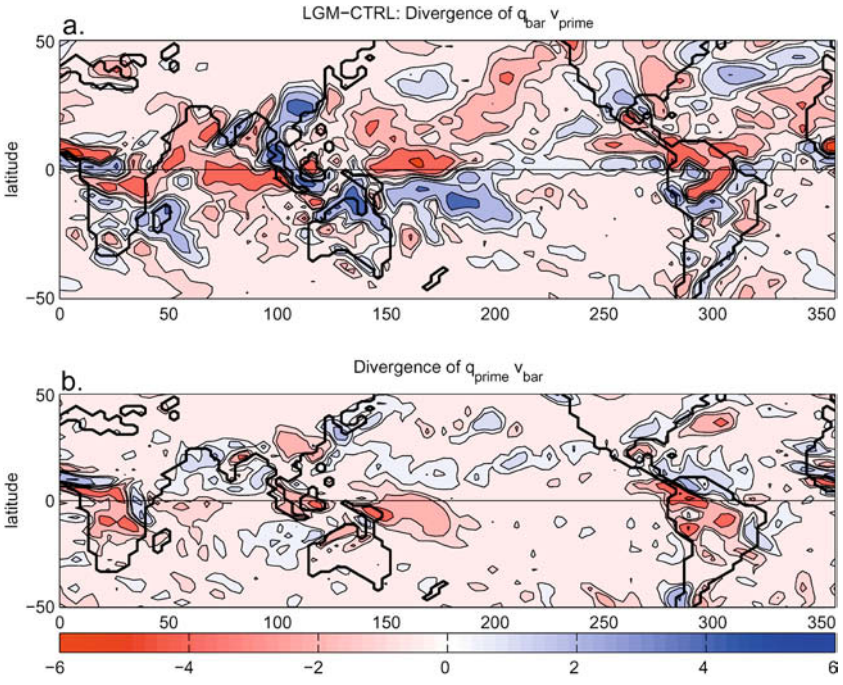

Fig. 7 **a** The DJF divergence of the anomalous advection of mean humidity (term II in Eq. 2) for LGM–CTRL in mm/day. **b** The DJF divergence of the mean advection of the anomalous humidity field (term III in Eq. 2) for LGM–CTRL. The *contour interval* is logarithmic with values. Positive values mean an increase in water vapor convergence (*blue*) and negative is a decrease (*red*) to be consistent with Fig. 5b

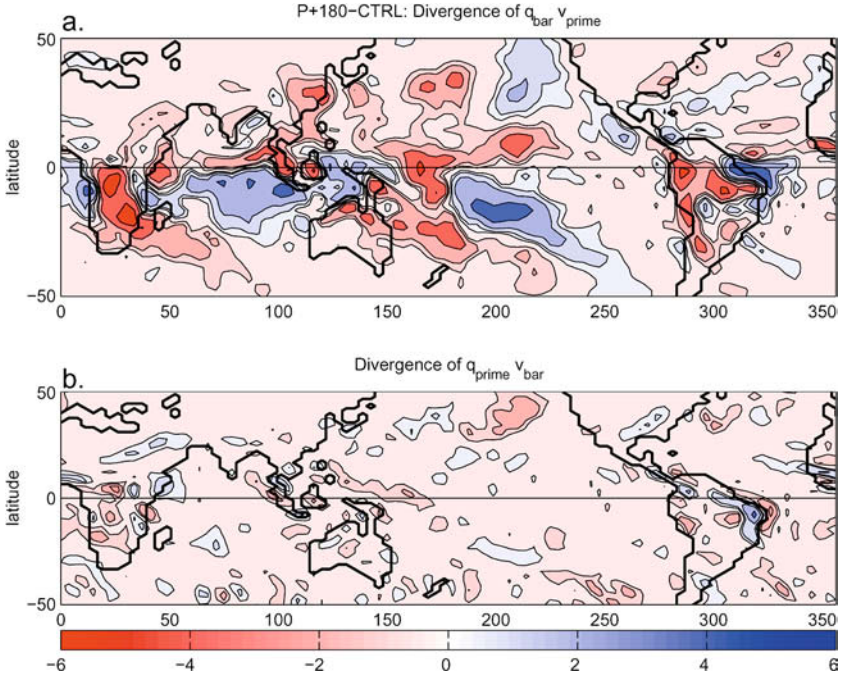

Fig. 8 **a** The DJF divergence of the anomalous advection of mean humidity (term II in Eq. 2) for P + 180–CTRL in mm/day. **b** The DJF divergence of the mean advection of the anomalous humidity field (term III in equation 2) for P + 180–CTRL. The *contour interval* is logarithmic with values. Positive values mean an increase in water vapor convergence (*blue*) and negative is a decrease (*red*) to be consistent with Fig. 5c

precession (Fig. 6c), resulting in little change in the humidity field.

4.3 The boreal summer response

Figures 9, 10, and 11 show the boreal summer response to the glacial and precessional forcing. The glacial forcing generates anomalous convergence in the upper troposphere over most of the northern tropics (Fig. 9b). There is a weakening of the JJA Hadley cell (Fig. 10b) due to the weaker contrast between the warm (Northern) and cold (Southern) Hemispheres consistent with the reduction in precipitation in the northern tropics in the latitude belt of the Hadley cell's rising branch. Figure 12 shows that, as in DJF, there is a significant contribution to the precipitation changes both by anomalous advection of the mean humidity field (term II in Eq. 2) and by mean advection of the anomalous humidity field (term III in Eq. 2). Again, the pattern shown in Fig. 12b agrees

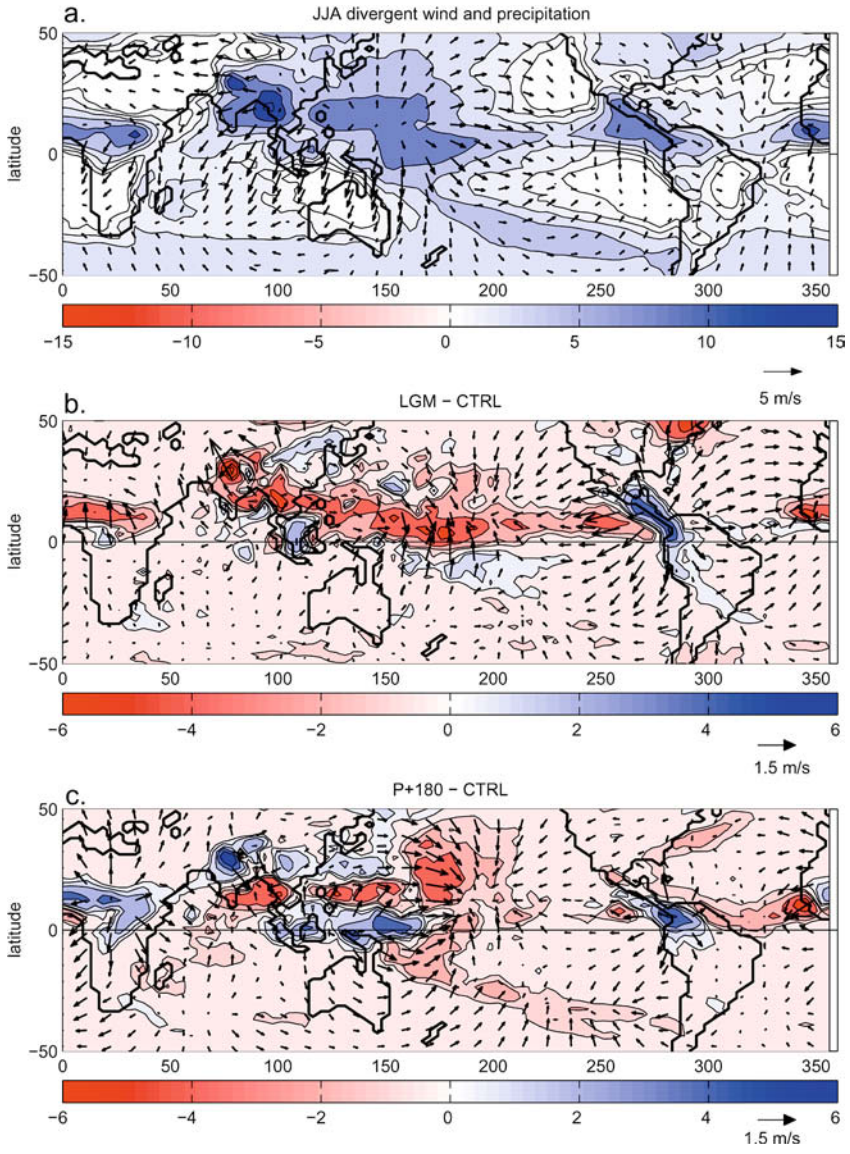

Fig. 9 JJA precipitation (*colors* and *contours*, mm/day) and upper tropospheric divergent winds (*vectors*, m/s) for **a** CTRL, **b**LGM–CTRL, **c** P + 180–CTRL. The *contour interval* for precipitation is logarithmic with values The zero contour is not drawn in all panels to improve clarity

well with the mean precipitation field shown in Fig. 9a. Thus, the glacial response in the precipitation field can be thought of as the combined effects of dynamics (a weaker Hadley circulation with reduced precipitation in the northern tropics) and thermodynamics (a reduction in the mean precipitation field).

The precessional response in the Northern Hemisphere summer circulation has significant zonal structure with little zonal mean change (Figs. 9c, 10c). Because of the stronger land-sea contrast, and stronger heating over Eurasia, the precipitation associated with the Asian monsoon is both strengthened and shifted to the north as has been discussed in previous studies (Kutzbach et al. 1977; Prell and Kutzbach 1987; Kutzbach and Liu 1997; Joussaume et al. 1999). The altered Asian monsoon has a clear response over the central North Pacific where there is upper tropospheric convergence and reduced precipitation. The pattern is very much like the response to diabatic heating over land as described by Rodwell and Hoskins (2001). There is an increase in the northern tropical easterlies over the oceans (not shown) which is part of a strengthening of the subtropical anticyclone, as was suggested by those authors. As in the DJF response to precession (Fig. 8), the precipitation changes are almost entirely explained by the circulation changes (not shown). In this season, however, since there is more incident solar radiation, there is a shift of precipitation from the ocean to the land in the Northern Hemisphere, which explains the pattern shown in Fig. 3b.

4.4 Summary

Three main points emerge from this study of the seasonal responses to the glacial and precessional forcing, all of which have implications for the interpretation of the paleoclimate record:

1. The response of the atmospheric circulation and hydrologic cycle to glacial and precessional forcing can be related in large part to changes in the zonal

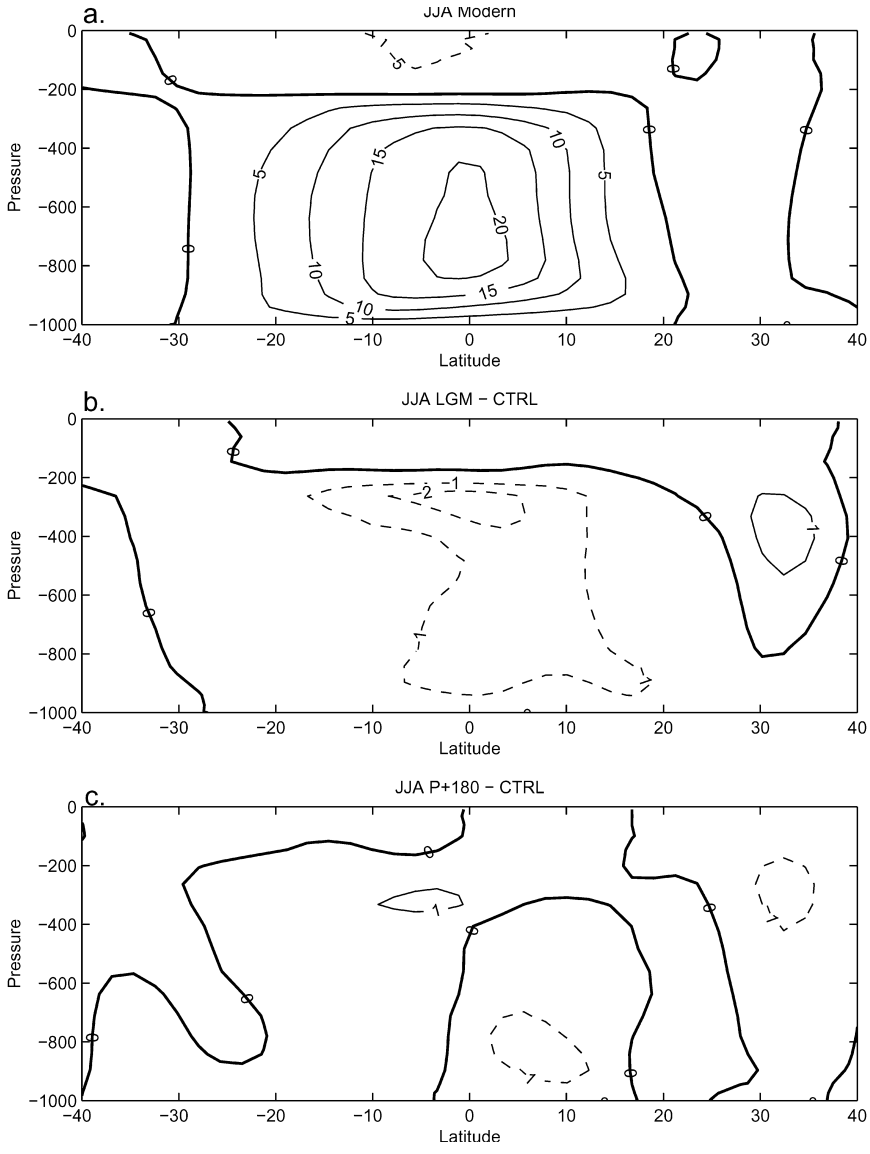

Fig. 10 JJA zonal mean meridional stream function (10^{10} kg/s) for **a**CTRL, **b** LGM–CTRL, **c** P + 180–CTRL

and meridional gradients of atmospheric heating. The circulation response to the changes in the heating gradients is governed by large-scale dynamical mechanisms, with rising motion and precipitation in one region often linked directly to sinking motion and dry conditions in another region. Because it is the changes in the gradients rather than absolute values of heating that are most relevant for the externally forced changes in the hydrologic cycle, regional temperature anomalies associated with these external forcings need not have the same sign as their counterparts in the precipitation field.

2. The mechanisms governing the response to glacial and precessional forcings are distinct. The glacial forcing strengthens the boreal winter Hadley cell, and weakens its boreal summer counterpart. This is due to a significant change in the meridional temperature gradient, with more cooling in the Northern Hemisphere than in the Southern Hemisphere. Local processes also play a role in the glacial response. Humidity is reduced everywhere in the cooler glacial climate, resulting in precipitation reductions in regions where precipitation is large in the unperturbed climate. The precessional response, on the other hand, has a zonally asymmetric structure stemming from the larger thermodynamic response to precessional forcing over land than ocean. This tends to shift precipitation from land to ocean when precessional forcing results in less sunshine in the tropics during a given season. Conversely, precipitation tends to shift from ocean to land when the tropics receive unusually large amounts of insolation at a particular time of year. Unlike the glacially forced changes in precipitation which result from both circulation and humidity anomalies, precipitation changes forced by precession are driven almost exclusively by changes in the circulation.

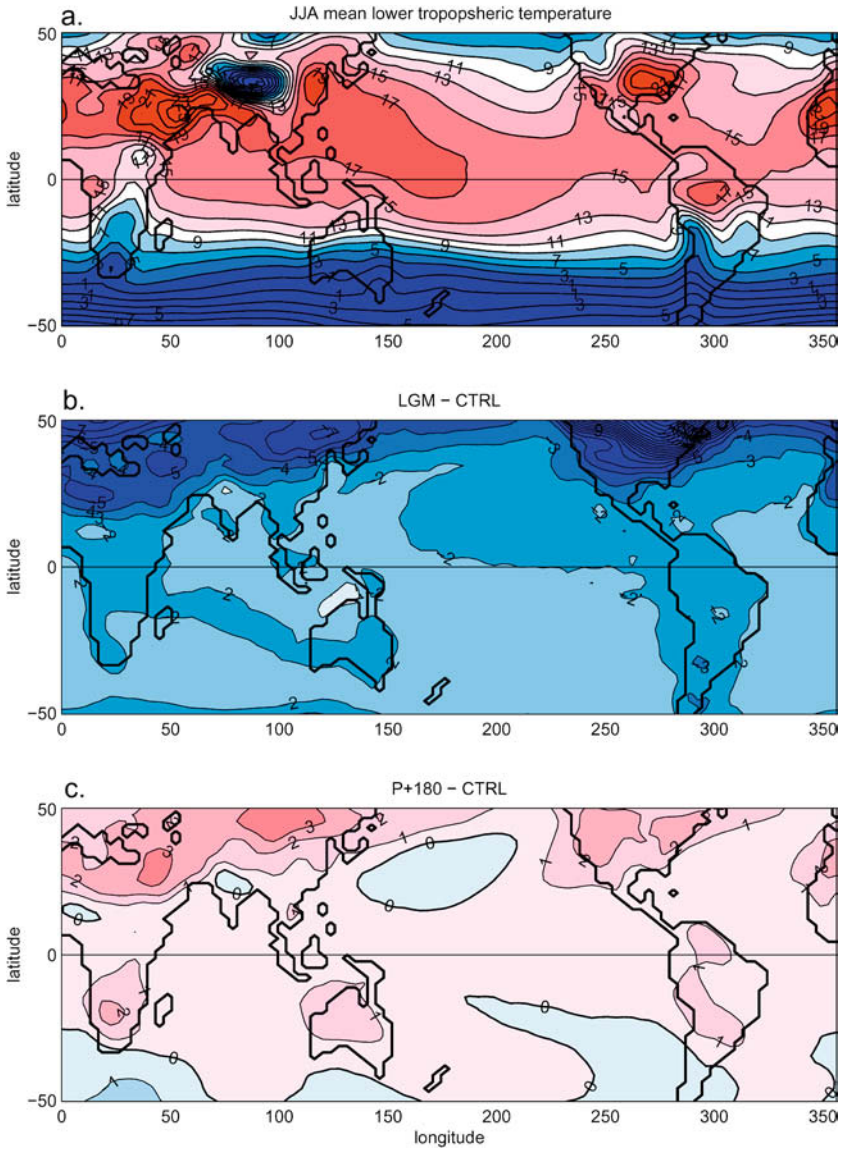

Fig. 11 JJA lower tropopsheric temperature (averaged over 1000–500 hPa) for **a** CTRL. *Contour interval* is 2 K. **b** LGM–CTRL, **c**P + 180–CTRL. The *contour interval* is 1 K in **b** and **c**

3. The annual mean temperature response to glacial forcing is more than an order of magnitude larger than the precessional response. However, because both the precessional and glacial forcings have significant impacts on the large-scale zonal and meridional gradients in atmospheric heating, the responses in the divergent circulation of the tropical atmosphere are comparable in magnitude. Thus, regional precessional signals in the hydrological cycle can be as large as their glacial counterparts in the tropics.

5 The absence of interactive ocean dynamics

A potential limitation of the current model arrangement is that it does not include interactive ocean dynamics, which are fundamental in establishing the mean climate of the tropics. If ocean dynamics were included, the model results shown here would no doubt be somewhat different, but our interpretation of them would probably not change. The atmospheric-mixed layer ocean response is the likely first-order response to the glacial and precessional forcing because it can be linked to very large changes in the meridional and zonal gradients of atmospheric heating. For example, the glacially driven change in the temperature contrast between the Northern and Southern Hemispheres is about 2 °C (from the equator to 50 degrees latitude). It is difficult to imagine an ocean dynamical mechanism that could generate a hemispheric temperature contrast large enough to overwhelm this signal. Clement and Seager (1999) and Seager et al. (2002) show that, even in the extreme case with no dynamical ocean heat transports at all, the change in zonal mean equator-to-pole temperature gradient in the Northern Hemisphere relative to the modern climatology is smaller than the glacial change simulated in our experiments.

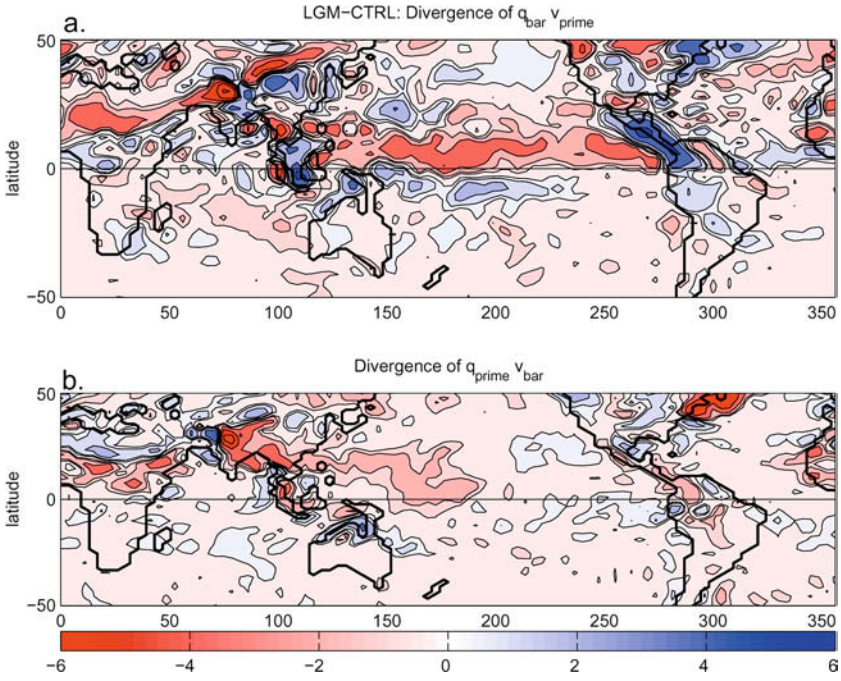

Fig. 12 **a** The JJA divergence of the anomalous advection of mean humidity (term II in Eq. 2) for LGM–CTRL in mm/day. **b** The JJA divergence of the mean advection of the anomalous humidity field (term III in Eq. 2) for LGM–CTRL. The *contour interval* is logarithmic with values The zero contour is not drawn in all panels to improve clarity. Positive values mean an increase in water vapor convergence (*blue*) and negative is a decrease (*red*) to be consistent with Fig. 11b

In the precessional case, the response in the circulation and precipitation fields is related to the land-sea temperature contrast. This too is on the order of several degrees, and is unlikely to be overwhelmed by oceanic processes. On interannual time scales, the tropical ocean is very effective at generating zonal asymmetries in the sea surface temperature (SST) as exemplified by the El Nino/Southern Oscillation. These zonal gradients can be several degrees in magnitude, and have a significant impact on the atmospheric circulation. However, ENSO is a transient phenomenon, and zonal gradients of this magnitude do not persist on the time scale of adjustment of the equatorial thermal structure, which is of the order of decades (Fine et al. 1987). There are ENSO-like changes in SST that persist on decadal time scales (Zhang et al. 1997), however, the zonal SST gradients associated with these changes are less than a degree. Thus, ocean dynamical mechanisms capable of generating persistent SST gradients are likely to be second order relative to the surface temperature gradient response to the glacial and precessional forcing simulated in our experiments.

More evidence for the secondary effects of ocean dynamics on the climate response to orbital forcing can be found in recent studies that quantify these effects explicitly (Kutzbach and Liu 1997; Otto-Bliesner 1999; Khodri et al. 2001). For example, Kutzbach and Liu (1997) showed that while interactive ocean physics contribute to an increase in the North African monsoon at 6 ka, the effect is only a 25% increase relative to the change due to atmosphere-only response to orbital forcing with SSTs fixed at modern values. The 25% increase includes the effect of both ocean mixed-layer physics (which is included in our model arrangement) and ocean dynamical adjustments, so the impact would likely have been even smaller if the authors had separated out the effect of the atmosphere-mixed layer interaction, and quantified only the effect of ocean dynamical adjustment. Recent studies investigating the role of the ocean in determining the sensitivity of the tropical climate to LGM boundary conditions produce mixed results. Hewitt et al. (2001) find generally the same sensitivity with and without ocean dynamics in the Hadley center coupled model, while Shin et al. (2003) find that ocean dynamics increase the tropical climate sensitivity in the NCAR coupled model. Thus, it is as yet unclear how much of a feedback ocean dynamics provide in the LGM climate.

6 Discussion

Because the glacial signal is so large in such phenomena as temperature, it has become common practice to place regional records everywhere on the same time scale as the global ice volume curve. Implicit in this practice is the assumption that local records are somehow correlated with the glacial signal, albeit with some possible phase differences. While this may be useful for temperature proxies, our results suggest that climate variability relating to the hydrological cycle may vary from region to region somewhat independently of global ice volume changes. Furthermore, the precipitation changes shown in Figs. 4 and 9 imply that regionally, the precessional signal can be as large as or larger than the glacial signal. Thus, when interpreting observed climate changes at specific locales and at specific times, it is important to have an a priori notion of how much of and in what way the signal can be attributed to glacial boundary conditions as opposed to precessional forcing.

Tropical ice cores provide an interesting example of a different interpretation of paleoclimate records supported by our results. Widespread depression of tropical snowlines in the late glacial has been generally attributed to lower atmospheric temperatures at the LGM (e.g., Porter 2001). Since tropical temperatures are lower everywhere largely due to reductions of CO_2(A.J. Broccoli personal communication), this reasoning implies that tropical glaciers should fluctuate roughly synchronously with the CO_2 changes and the high-latitude ice sheets. However, Thompson et al. (2002) point out that there is substantial asynchrony in the fluctuations of tropical glaciers at various locations. In Tibet, the date of the base of the Dasuopu ice core is 9 ka (Thompson et al. 2002b) and on Mt. Kilimanjaro it is 11 ka (Thompson et al. 2002c). In contrast, in the Andes, the Huascaran glacier dates to 19 ka (Thompson et al. 1995) while the Sajama ice core dates to 25 ka (Thompson et al. 1998). The assumption of synchrony in tropical glaciation can be challenged on the grounds that changes in accumulation have not been fully taken into account. Since the mass balance of glaciers is determined not only by changes in ablation (largely controlled by temperature and insolation), but also accumulation, changes in the hydrologic can play an important role. Examining Figs. 4 and 9, it is clear that if hydrological controls on glacier mass balance are important, the history of tropical glaciers can be quite distinct from that of the high latitudes. This point is further supported by lake records from throughout the tropics, which can be entirely dominated by precession (Gasse 2000; Bush et al. 2002; Trauth et al. 2003).

Our results also illustrate the impossibility of adopting a purely local perspective to understanding the climate system's response to precessional forcing. As we show in Sect. 4, the response in the atmospheric circulation and hydrologic cycle is related to large-scale temperature gradients, linking wide regions of the tropics. Since the precessional forcing has the effect of shifting regions of precipitation around, there is no simple rule of thumb for how the signal may appear locally. Consider the precessional precipitation signal over the subtropical North Pacific in JJA (Fig. 9c). In that season, there is reduced precipitation, while Fig. 11cshows that the lower tropospheric temperature is warmer than modern. From a strictly local analysis, one might have expected that increased solar radiation would be associated with wetter conditions locally, as is often assumed. However, because conditions over the North Pacific Ocean are related to the remote response to the Asian monsoon, warmer surface temperatures are associated with drier conditions in that region. With new techniques in generating oceanic proxies of salinity change (e.g., Lea et al. 2000), it will be possible to unravel these hydrologic signals over the ocean, which are a fundamental part of the tropical climate response to external forcing.

In this work, we have not considered the influence of obliquity forcing in the tropics. Because obliquity variations affect annual mean insolation, there is a significant response in annual mean temperature (Jackson and Broccoli 2003). Also, because obliquity influences the meridional gradient of annual mean insolation (for high obliquity, the poles receive relatively more radiation and the tropics less), it is likely that there would be a response in the mean meridional circulation with some influence on the hydrologic cycle. There is some indication of an obliquity signal in the hydrologic cycle from paleoceanographic records (Cortijo et al. 1999), and there is an active debate as to the role of obliquity in late Quaternary climate change (Paillard 2001; Raymo and Nisancioglu 2003). Presently, the relative influence of obliquity, precession and glacial forcing has not been quantified, and further studies with GCMs are necessary to address this issue. Nevertheless, obliquity forcing represents another source of variability in the tropics, with what is likely to be both a distinct signal and a distinct mechanism. Obliquity variations would be likely to add to the orbitally induced climate variability that has been simulated in the current experiments, and thus increase the fraction of tropical climate variability that can be directly related to orbital forcing.

In summary, we submit that while much attention in the past has focused on explaining the global changes associated with the glacial-interglacial cycle, deciphering the precessional signals is also important to understanding the history of the tropical climate. The mechanisms we discuss here can provide guidance in understanding the regional sensitivity of climate, and in linking records from different parts of the tropics. Our results also suggest the record of hydrologic changes may contain important information about the fundamental behavior of the tropical climate.

Acknowledgements The authors wish to thank Claes Rooth, Mark Maslin and two anonymous reviewers for their comments. A.C was supported by National Science Foundation CAREER grant #ATM-0134742 and National Science Foundation grant #ATM-9986515. A.H. was supported by National Science Foundation CAREER grant ATM-0135136. A.J.B was supported by New Jersey Agricultural Experiment Station Project NJ07167.

References

Berger AL (1978) Long-term variations of daily insolation and quaternary climate changes. J Atmos Sci 35: 2362–2367

Broccoli AJ (2000) Tropical cooling at the last glacial maximum: an atmosphere-mixed layer ocean model simulation. J Clim 13: 951–976

Broccoli A, Manabe S (1987) The influence of continental ice, atmospheric CO_2 and land albedo on the climate of the Last Glacial Maximum. Clim Dyn 1: 87–99

Broecker WS (1995) The glacial world according to Wally. 318 pp., Lamont-Doherty Earth Observatory, Palisades, NY, USA

Bush M, Miller MC, de Oliveira P, Colinvaux P (2002) Orbital-forcing signal in sediment of two Amazonian lakes. J Paleolim 27: 341–352

Chen P, Hoerling M, Dole R (2001) The origin of the subtropical anticyclones. J Atmos Sci 58: 1827–1835

Clement AC, Seager R (1999) Climate and the tropical oceans. J Clim 12: 3384–3401

Cortijo E, Lehman S, Keigwin L, Chapman M, Paillard D, Labeyrie L (1999) Changes in meridional temperature and salinity gradients in the North Atlantic Ocean (30–72N) during the Last Interglacial Period. Paleoceanology. 14: 23–33

Fine RA, Peterson WH, Ostlund HG (1987) The penetration of tritium into the tropical Pacific. J Phys Oceanogr 5: 553–564

Ganopolski A, Rahmstorf S, Petoukov V, Claussen M (1998) Simulation of modern and glacial climate with a coupled global model of intermediate complexity. Nature 391: 351–356

Gasse F (2000) Hydrological changes in the African tropics since the Last Glacial Maximum. Quat Sci Rev 19: 189–211

Hall A (2003) Role of surface albedo feedback in climate. Part I: internal climate variability. J Clim (in press)

Hall A, Manabe S (2000) The effect of water vapor feedback on internal and anthropogenic variations of the global hydrologic cycle. J Geophys Res 105: 6935–6944

Harrison SP, Kutzbach JE, Prentice IC, Behling JP, Sykes MT (1995) The response of Northern Hemisphere extratropical climate and vegetation to orbitally induced changes in insolation during the Last Interglaciation. Quat Res 43: 174–184

Hays JD, Imbrie J, Shackleton NJ (1976) Variations in the Earth's orbit: pacemaker of the ice ages. Science 194: 1121–1132

Hewitt CD, Mitchell JFB (1997) Radiative forcing and response of a GCM to ice age boundary conditions: cloud feedback and climate sensitivity. Clim Dyn 13: 821–834

Hewitt CD, Broccoli AJ, Mitchell JFB, Stouffer RJ (2001) A coupled model study of the last glacial maximum: was part of the North Atlantic relatively warm? Geophys Res Lett 28: 1571–1574

Imbrie J et al (1984) The orbital theory of Pleistocene climate: support from a revised chronology of the marine $\delta^{18}O$ record. In: Berger AL et al. (eds) Milankovich and climate. Reidel, Hingham, MA, USA, pp 269–305

Imbrie J et al (1992) On the structure and origin of major glaciation cycles, 1, linear responses to Milankovitch forcing. Paleoceanography 7: 701–738

Imbrie J et al. (1993) On the stucture and origin of major glaciation cycles, 2, the 100,000-year cycle. Paleoceanography 8: 699–735

Jackson CS, Broccoli AJ (2003) Orbital forcing of the Arctic climate: mechanisms of climate response and implications for continental glaciation. Clim Dyn (in press)

Joussaume S et al (1999) Monsoon changes for 6000 years ago: results of 18 simulations from the Paleoclimate Modeling Intercomparison Project (PMIP). Geophys Res Lett 26: 859–862

Joussaume S, Braconnot P (1997) Sensitivity of paleoclimate simulation results to the season definitions. J Geophys Res 102: 1943–1956

Joussaume S, Taylor K (1995) Status of the paleoclimate modeling intercomparison project (PMIP). In: Gates WL (ed) WCRP, pp 425–430

Khodri M, Leclainche Y, Ramstein G, Braconnot P, Marti O, Cortijo E (2001) Simulating the amplification of orbital forcing by ocean feedbacks in the last glaciation. Nature 410: 570–574

Kutzbach JE, Chervin RM, Houghton DD (1977) Response of the NCAR general circulation model prescribed changes in ocean surface temperature. Part I: mid-latitude changes. J Atmos Sci 34: 1200–1213

Kutzbach JE, Liu Z (1997) Response of the African monsoon to orbital forcing and ocean feedbacks in the middle Holocene. Science 278: 440–443

Lea DW, Pak DK, Spero HJ (2000) Climate impact of late Quaternary equatorial Pacific sea surface temperature variations. Science 289: 1719–1724

Lindzen RS, Hou AY (1988) Hadley circulations for zonally averaged heating centered off the equator. J Atmos Sci 45: 2416–2427

Lindzen RS, Pan W (1994) A note on orbital control of equator-pole heat fluxes. Clim Dyn 10: 49–57

Manabe S, Stouffer RJ (1980) Sensitivity of a global climate model to an increase of CO_2 concentration in the atmosphere. J Geophys Res 85C10: 5529–5554

Manabe S, Wetherald RT (1975) The effects of doubling CO_2 concentration on the climate of a general circulation model. J Atmos Sci 32: 3–15

Milankovitch M (1920) Theorie Mathematique des Phenomenes Produits par la Radiation Solaire. Gauthier-Villars, Paris, France

Mitchell JFB, Johns TC, Gregory JM, Tett SFB (1995) Climate response to increasing levels of greenhouse gases and sulfate aerosols. Nature 376: 501–504

Otto-Bliesner BL (1999) El Nino/La Nina and Sahel precipitation during the middle Holocene. Geophys Res Lett 26: 87–90

Paillard D (2001) Glacial cycles: toward a new paradigm. Rev Geophys 39: 325–346

Peltier W (1993) Time dependent topography through a glacial cycle. IGBP PAGES/World Data Paleoclimatology Program, Boulder CO, USA

Phillipps PJ, Held IM (1994) The response to orbital perturbations in an atmospheric model coupled to a slab ocean. J Clim 7: 767–782

Pinot S et al (1999) Tropical paleoclimates at the Last Glacial Maximum: comparison of Paleoclimate Modeling Intercomparison Project (PMIP) simulations and paleodata. Clim Dyn 15: 857–874

Porter SC (2001) Snowline depression in the tropics during the Last Glaciation. Quat Sci Rev 20: 1067–1091

Prell WL, Kutzbach JE (1987) Monsoon variability over the last 150,000 years. J Geophys Res 92: 8411–8425

Raymo M, Nisancioglu K (2003) The 41 kyr world: Milankovitch's other unsolved mystery. Paleoceanography 18, doi: 10.1029/2002PA000791

Rind D, Peteet D, Kukla G (1989) Can Milankovich orbital variations initiate the growth of ice sheets in a general circulation model? J Geophys Res 94: 12,851–12,871

Rodwell MJ, Hoskins BJ (1996) Monsoons and the dynamics of deserts. Q J R Meteorol Soc 122: 1385–1404

Rodwell MR, Hoskins BJ (2001) Subtropical anticyclones and monsoons. J Clim 14: 3192–3211

Seager R et al (2002) Is the Gulf Stream responsible for Europe's mild winters? Q J R Meteorol Soc 28: 2563–2586

Shackleton NJ (2000) The 100,000-year ice-age cycle identified and found to lag temperature, carbon dioxide and orbital eccentricity. Science 289: 1897–1902

Shin SI, Liu Z, Otto-Bliesner BL, Brady EC, Kutzbach JE, Harrison SP (2003) A simulation of the Last Glacial Maximum climate using NCAR-CCSM. Clim Dyn (in press)

Thompson LG et al (1998) A 25,000-year tropical climate history from Bolivian ice cores. Science 282: 1858–1864

Thompson LG, Mosley-Thompson E, Lin P-N, Mashiotta TA (2002a) Ice core evidence of past changes in the hydrological cycle of the tropics and subtropics. Eos Trans, AGU, Fall Meeting Suppl 83: Abstr PP61B-02

Thompson LG et al (2002b) Holocene climate change in the tropics: evidence of abrupt climate change past and present. Nature (in press)

Thompson LG et al (2002c) Kilamanjaro ice core records: evidence of Holocene climate change in tropical Africa. Science 298: 589–593

Thompson LG et al (1995) Late glacial stage and Holocene tropical ice core records from Huascaran, Peru. Science 269: 46–50

Trauth M, Denino A, Bergner A, Strecker M (2003) East African climate change and orbital forcing during the last 175 kyr BP. EPSL 206: 297–313

Trenberth KE, Stepaniak DP, Caron JM (2000) The global monsoon as seen through the divergent atmosheric circulation. J Clim 13

Zhang Y, Wallace JM, Battisti DS (1997) ENSO-like decade-to-century scale variability: 1900–93. J Clim 10: 1004–1020